Effect of underwater lighting on observations of density and behavior of rockfish during camera surveys

Christopher N. Rooper [1 *], Kresimir Williams [1], Alex DeRobertis [1], Vanessa Tuttle [2]

[1] Alaska Fisheries Science Center, National Marine Fisheries Service, NOAA

7600 Sand Point Way NE

Seattle WA 98115

[2] Northwest Fisheries Science Center, National Marine Fisheries Service, NOAA

2725 Montlake Blvd. East

Seattle WA 98112-2097

[*] Corresponding author information :

Telephone: 206-526-4689

Email: chris.rooper@noaa.gov

Abstract:
Unbiased visual observations of fish are increasingly important for a number of management issues, such as non-extractive abundance estimates and fish-habitat associations. We tested the effect of three types of underwater lighting on observable rockfish density and behavior using an underwater stereo camera. Higher densities of small rockfish were observed on deployments conducted with strobed red lights (where rockfish are less spectrally sensitive) than with either strobed white light or constant white light. The difference between strobed red lights and constant white light was statistically significant. For three larger species of rockfish there was no significant effect of lighting on fish density. Rockfish behavioral responses measured by the range-dependent height off the seafloor were also lowest for the red strobe light deployments, although not significantly different than for white strobe light. Rockfish height above the seafloor decreased as the drop camera approached in all treatments for both small and large rockfish. Small rockfish exhibited stronger responses to light treatments both in terms of density and observed height off the seafloor, while large rockfish were less sensitive to any of the light treatments. The implications of this study are that white lights decrease the observed density of small rockfish during underwater surveys, and the degree to which lighting regimes overlap the spectral sensitivities of target fishes can determine fish reactions.

Keywords:
Underwater stereo imagery, underwater lighting, Sebastes, visual surveys, habitat studies, Puget Sound

1.1 Introduction

Visual surveys for marine fishes have become more prevalent in recent years with the development and accessibility of new technologies (such as stereo image processing), the desire by management agencies to conduct non-extractive studies (for rare or endangered species), and the need to survey fishes in areas where traditional sampling gears are not appropriate (such as untrawlable rocky areas). Underwater imagery has been commonly used to assess fish associations with their habitat (Hixon et al. 1991; Stein et al. 1992; Auster et al. 2003; Love et al. 2009) and less commonly used to estimate fish abundance using non-lethal methods (O'Connell and Carlile 1993; Yoklavich et al. 2007). More recently, underwater imagery has been used in combination with other methods such as acoustics to estimate population abundance of difficult to assess species (Demer et al. 2009; Ressler et al. 2009; Rooper et al. 2010; Jones et al. 2012). To a large degree, all of these applications of underwater visual observations depend on unbiased estimates of fish species composition, fish abundance and fish sizes in different habitats, yet the effect of the observation platform on the observations are rarely measured (see review by Stoner et al. 2008).

Underwater platforms for visually assessing fish-habitat associations and fish abundance have included basic systems such as drop cameras (Rooper et al. 2010; Jones et al. 2012), remotely operated vehicles (O'Connell and Carlile 1994; Stone 2006; Steirhoff et al. 2013) and manned submersible vehicles (O'Connell and Carlile 1993; Yoklavich et al. 2007). Stimuli associated with underwater platforms can include artificial lighting, underwater platform noise, water displacement from platform motion, platform speed, chemical or electromechanical stimuli (Stoner et al. 2008), and stimuli from the underwater plotform support vessel (De Robertis and Handegard 2013). In the few studies that have been conducted, the effect of an underwater platform on the behavior of fishes is often found to vary with species (Trenkel et al. 2004; Lauth et al. 2004; Laidig et al. 2013). Rockfish (*Sebastes* spp.) are a taxonomic group that is often the subject of visual surveys due to their predisposition to occur near the seafloor in rocky or rough areas where other types of sampling (such as trawls or set nets) are ineffective. Field studies of rockfish have observed differential reactions to underwater platforms, including diving to the seafloor, changing the speed or direction of swimming, following the platform, or limited reaction to the platform (Pearcy et al. 1989; Hixon et al. 1991; Krieger and Ito 1999; Lauth et al. 2004; Lorance and Trenkel 2006; Laidig et al. 2013), indicating there could be potential biases in abundance estimates associated with fish reactions to the observation platforms during visual surveys.

The artificial lighting associated with underwater visual platforms is often considered to be the predominant source of disturbance and potential bias for fishes during visual surveys (Stoner et al. 2008). However, the effects of different lighting regimes on fish avoidance behavior have only rarely been studied. A single published laboratory study by Ryer et al. (2009) examined the effects of the approach of artificial lighting on seven marine fish species, and found that reactions to the light varied among them. Few field studies have examined the effect of lighting on the abundance of observed fishes. Widder et al. (2005) found that the number of sablefish (*Anoplopoma fimbria*) observed was higher when illumination was provided with red as opposed to white lights, and Trenkel et al. (2004) found an increase in white light intensity resulted in a decrease of observed fishes. In general, fish vision is sensitive to light wavelengths in the range of blue (400 nm) to far-red (700 nm) (Bowmaker 1990; Douglas and Hawryshyn 1990). A study on black rockfish (*Sebastes melanops*) indicates they are sensitive to light in the range from 380 nm to 620 nm (Brill et al. 2008) In a laboratory study, it was found that rockfish reaction to white light from an incandescent source was generally moderate, but varied with species (Ryer et al. 2009). Based on the review of Stoner et al. (2009) and research of Ryer et al. (2009), we expected that the rockfish exposed to light that fell within the wavelengths of high sensitivity would have an avoidance reaction to the camera, either by moving away from the camera prior to their being observed (causing a decrease in observed density) or by moving towards the refuge of seafloor (causing an observed decrease in height above the seafloor).

Thus, the objectives of this study were to determine the effects of three lighting treatments on the abundance of rockfish observed with a drop camera in terms of rockfish density and maximum number observed. Where species of rockfish could be determined, differences in abundance were compared among species. A secondary objective was to examine rockfish avoidance (measured by changes in density) with distance from the drop camera, and rockfish behavior (measured by the height of rockfish off the seafloor) under the three lighting treatments. Where possible, these comparisons were also made among species.

2.1 Material and Methods

This study was conducted from November 18 to 22, 2013 in the San Juan Islands near Friday Harbor, Washington (Fig. 1). The University of Washington research vessel *Centennial* was used for all operations. Maps of seafloor substrates have been completed for much of the San Juan Archipelago (Greene et al. 2007) that show areas of potential hard rocky substrate. Surveys with remotely operated vehicles have also been conducted in the area, which indicated potential areas of high rockfish concentration (R. Pacunski, Washington Department of Fish and Wildlife, 600 Capitol Way N., Olympia, WA 98501, U.S.A., personal communication). Based on initial explorations using the ships echosounder, drop camera system, previous rockfish sightings and the seafloor substrate maps, 11 transects were chosen (Fig. 1). The 11 transects ranged in depth from 36 m to 69 m (mean = 54 m, SE = 1.6).

2.2 Drop camera system

The drop camera system used in this study was similar to that described in Williams et al. (2010). The drop camera is designed to be towed or drifted continuously along a linear transect at or near the seafloor, rather than a camera that is lowered to the seafloor at one position and then brought immediately to the surface or lowered to the seafloor and anchored during an observation period. The electronic components of the drop camera were protected by a cage constructed from aluminum tubing (Fig. 2a). Two machine-vision cameras (a JAI AB-201GE and a JAI CM-140GE) spaced 30 cm apart in underwater housings were connected via underwater ethernet cables to a computer in a 12.7 cm (5 inch) diameter housing. The camera on the right side recorded monochromatic still images sized at 1.45 megapixels, while the camera on the left side collected 1.73 megapixel color still images. The computer, cameras and lights were powered by a 28 V NiMH battery pack. Synchronous images were collected from each of the cameras at a frequency of one image per second and written to a hard drive on the computer. Additionally, images were taken (but not written to the hard drive) from the monochrome camera at a rate of four images per second. These images were viewed in real time on a monitor at the surface. This allowed the height of the camera to be actively controlled to keep it just above the seafloor using a quick response electric winch (Fig. 2b). A 3/16 inch diameter coaxial cable provided the connection from the drop camera system to the winch at the surface and allowed image viewing in real time. A small-diameter cable was used to minimize drag on the drop camera system and to minimize fish responses to the deployment cable. During each deployment, the drop camera system was towed through the water column at a speed of 1.85 to 3.70 km*hr^{-1} (1 to 2 knots) approximately 1 to 2 m above the substrate with the cameras pointed slightly downward at an angle of approximately 35° off parallel to the seafloor. The tow duration averaged 15 minutes and ranged from about 8 minutes to 25 minutes.

2.3 Lighting treatments

The lighting treatments consisted of a red strobed light (RS, control), white strobed light (WS), and a continuous white light (CW). Each of four RS lights attached to the drop camera consisted of eight 2.1 W 660 nm LED Engin® High Power LEDs controlled by a single TaskLED® driver, while the four WS lights were constructed of four Bridgelux® BXRA LED arrays capable of producing 1,300 lumens at 10.4 W. The CW lights deployed on the drop camera system consisted of a combination of one DeepSea Power & Light SeaLite® Sphere constant LED white light and one 50 W high-intensity discharge (HID) light (Fig. 2c). Light intensity perceived by the fish was not measured directly, as it was impossible to estimate due to different exposure times, attenuation, spectral sensitivity and strobe spread, all of which varied somewhat among the different lights. We set up the lighting parameters to achieve a reasonable exposure in the field, meaning for the camera, the light "intensity" was roughly the same among treatments. The strobed lights were all triggered at a rate of four times per second.

The absorption coefficient of light at wavelengths less than 350 nm and greater than 750 nm is very high (Fig. 3), effectively limiting the distance at which objects can be observed. The spectral sensitivity of adult black rockfish (*Sebastes melanops*) has previously been shown to peak at about 500 nm, with a range from ~380 nm to ~620 nm (Brill et al. 2008). The red strobe light emitted in a narrow band from approximately 640 to 680 nm (Fig. 2), thus it was not expected to be conspicuous to the rockfish. The white LED strobe and LED constant lights used in this experiment emitted throughout the entire rockfish spectral sensitivity range, but exhibited a fairly narrow peak at about 450 nm and a much lower but broader peak at 550 nm. The HID light emitted across a broad range, from approximately 400 to > 800 nm with a peak at 620 nm (Fig. 2). Treatments were applied in a random order.

2.4 Stereo image analysis

The drop camera system was calibrated in a test tank using a stereo camera calibration procedure with a calibration checkerboard according to the methods of Bouguet (2008) and Williams et al. (2010). The calibration resulted in a correction for lens distortion and solution for the epipolar geometry by iteratively solving for the translation and rotation vectors that describe the relationship between the coordinate systems of the two cameras (Xu and Zhang, 1996). Once these matrices were estimated, the three-dimensional position of a target point viewed in both cameras could be determined by stereo-triangulation. Measurements were made using stereo-triangulation functions supplied with the camera calibration software package written in the Matlab computing language (Bouguet, 2008; V R2010, Mathworks Inc.).

Fish lengths were obtained by identifying the pixel coordinates of corresponding points (such as a fish snout or tail) seen in the left and right camera still frames. These points were used to solve for the three-dimensional coordinates of the points in the images by triangulation, by using the calibration-derived parameters. In addition to length measurements, the three-dimensional coordinates extracted from the still-frame images provided data on the position and orientation of objects relative to the camera. These data were used to determine distances of fish targets to the seafloor, distances of fish and other targets from the camera and the orientation of fish (Fig. 4).

Each stereo image pair was classified into one of two habitat classifications based on the presence of rocky substrate. Images where bedrock, boulders or cobble were present were classified as rocky habitat. Images where only sand, gravel or mud was observed were classified as soft. For each image frame (taken at a rate of one per second) the number of fish observed by species was counted. All rockfish where the fish snout and tail were visible in both cameras were measured for length using stereo techniques. For these fish, the range (distance from the camera) and the orientation relative to the camera (direction in which the fish was headed) were computed. For fish that appeared in both images, but both the nose and tail did not appear, or they were otherwise unmeasurable, a range to the fish was calculated. Typically, for these fish if the eye was visible in both images, it was used as the target for ranging. However, if another feature on the body of the fish was observable in both images, such as a stripe or fin, these features were used to measure the range. Fish that were in the field of view of only one camera were counted but could not be measured or ranged.

Fish counts per frame were converted to volumetric densities using the calculated geometry of each camera's field of view. The volume of overlapping field of view was estimated from the relative distance and orientation of the cameras. The range-dependent imaging volume was computed by modeling the camera field-of-view as a pyramidal shape defined by the vertical and horizontal view angles (Fig. 5). The joint volume viewed by both cameras was computed by combining the individual camera imaging pyramids with the translation and rotation matrix derived from the stereo calibration to produce a three-dimensional model of the viewing area (Fig. 5). The volume of the overlapping section was computed using

MATLAB software function for calculating volumes of arbitrary polygonal solids (geom3d package). The joint camera volume followed a 3rd order polynomial relationship with increasing range (Fig. 5).

The total volume observed was calculated as the sum of the individual camera volumes at maximum observable range *r* with the overlapping volume subtracted. The value of *r* varied with visibility conditions and was determined for each deployment by averaging the range to five farthest observable objects seen in both cameras.

For each deployment, identifiable objects visible in both cameras in successive frames were ranged to calculate how much the camera moved from frame to frame. This value was then used to weight the number of fish (*N*) observed in a frame (*i*), as

$$\widetilde{N}_i = \frac{N_i}{V_i} d_i$$

where $\widetilde{N}_i$ is the relative density of fish, V_i is the sample volume of the camera (at a range of *r*) and d_i is the distance traveled by the drop camera system (m) in successive frames (frame *i*-1 to frame *i*). If the drop camera system moved a large distance between frames, this was reflected in a higher relative density of fish observed per frame. If the camera did not move between successive frames, than $d = 0$, resulting in a density measurement of 0 for the successive frame. The value of *r* for each deployment was not significantly different among light treatments (p = 0.06), with WS lights achieving the farthest observable range (252 cm). The shortest observable distance was for the RS lights at 225 cm (Table 1).

2.5 Experimental design and analysis

The experiment was conducted following a randomized block design. At each of the 11 transects, 3 successive deployments were conducted, each with one of the lighting treatments

(RS, WS, CW). The treatment order was chosen at random for each of the 11 transects. The three successive deployments (each with a different lighting treatment) at a transect were used as a block, so that transect number (1-11) was used as a blocking variable (or factor) in the analysis. A randomized block analysis of variance (ANOVA) was used to analyze the densities of rockfish in two groups, large rockfish and small rockfish. The large rockfish species were Quillback Rockfish (*Sebastes maliger*), Copper Rockfish (*S. caurinus*), Yelloweye Rockfish (*S. ruberrimus*) and Vermillion Rockfish (*S. miniatus*). Small rockfish (< 20 cm) included large numbers of unidentified rockfish and Puget Sound Rockfish (*S. emphaeus*). The small rockfish category probably also contained juveniles of larger species (including those found in the large rockfish category).

The density and maximum number of rockfish data were analyzed in a 2-way ANOVA design with each deployment used as a sample unit ($n = 33$), and the transect where the three light treatments were sequentially deployed ($n=11$) was used a blocking variable. The mean density on a given deployment and the maximum number of rockfish observed in any frame on a deployment were used as dependent variables in separate ANOVA's to test for significant differences among light treatments. Significance for all analyses was judged at $p < 0.05$. Tukey's honest significant differences test (Tukey's HSD) was used as a post-hoc test for significant differences among levels of treatment. All analyses were completed in R software (R Core Development Team 2013).

The randomized block experimental design of three successive drop camera deployments each using a different lighting configuration was intended to control for the impacts of variables other than the lighting treatments. The goal was to follow an equivalent path over ground during each of the three sequential deployments with all three lighting treatments. Thus, the variability in density introduced by unmeasured variables, such as water temperature, ambient light, turbidity and current speed would cause a minimal effect on measured rockfish density. Water depth and the percentage of hard substrate were measured during each deployment. These variables did not vary significantly among the lighting treatments within a block ($p = 0.28$ for the percentage of hard substrate among treatments and $p = 0.46$ for the average depth among treatments) confirming that the statistical design was appropriate. Across blocks, these metrics were found to vary significantly ($p < 0.05$).

Rockfish avoidance behavior relative to the camera was assessed by the relationship of fish density relative to the distance from the camera. The hypothesis tested was that densities would not change as the camera approached. Alternatively, if fish exhibited a strong avoidance reaction to the approach of the camera, it was expected that densities would decrease as the camera approached. This hypothesis was tested for the large and small fish groupings separately using ANOVA. In the ANOVA, density for each transect where small or large rockfish occurred was calculated for each 25 cm bins from 50 cm to 200 cm away from the camera. This was used as the dependent variable. The distance bin, a treatment term and the block term, as well as the distance*treatment interaction term were used as independent variables.

The distance of the rockfish above the seafloor was also considered as a behavioral response to the approach of the drop camera system. In this analysis, 100 individuals from the small rockfish category for each treatment were chosen at random and their height above the seafloor was measured. For the large rockfish category there were fewer individuals recorded, so all height above bottom data was used. For each individual, the minimum distance from the rockfish to the seafloor was measured, by identifying the closest point on the rockfish to the seafloor and measuring the distance of that point to the nearest point on the seafloor using the calibrated stereo triangulation (Fig. 4). An analysis of covariance (ANCOVA) was used to test for significant differences between light treatments for height above the seafloor. In addition to the treatment effect, distance from the camera to the fish was used as a covariate in the analysis. The interaction term (treatment*distance) was also included in the analysis.

3.1 Results

Small rockfish were the most commonly observed fish along the transects in the camera drops, regardless of the type of illumination used (Table 2). Most of the small rockfish were classified as unidentified, but those that were identified to species were predominantly Puget Sound Rockfish. Large rockfish were predominantly copper and quillback rockfish. Most of the small rockfish (89%) and large rockfish (96%) were found in rocky or hard habitats. Rocky or hard habitats comprised 53% of the total images collected during all deployments. A variety of other species of fish were also observed during deployments including hexagrammids (Lingcod, Kelp Greenling and unidentified greenling), forage fish, such as unidentified gadids and Pacific Herring. Only rockfish were considered in the analyses.

The densities of small rockfish were significantly different among light treatments ($p = 0.005$, Table 3), with the highest densities observed under the RS treatment and lowest for the CW (Fig. 6). The post-hoc test indicated that both the RS and WS densities were significantly higher than the CW density; however, there was no significant difference between the RS and WS treatments. For large rockfish, there were no significant differences in densities observed among treatments ($p = 0.523$, Fig. 6, Table 3). Separate ANOVA's testing for an effect of order (i.e. a decrease in abundance after the initial pass through the transect irrespective of treatment) were not significant for either small rockfish (p = 0.42) or large rockfish (p = 0.73).

The maximum number of rockfish (both large and small combined) per frame averaged 11.3 fish (SE = 2.4) for RS, 7.3 fish (SE = 1.1) for WS and 4.3 fish (SE = 0.9) for the CW (Fig. 7). The ANOVA revealed that there were significant differences among treatments (p = 0.002, Table 3). The post-hoc test indicated that densities under the RS treatments were significantly higher than in the CW treatments.

The ANOVA comparing the density or small rockfish as a function of light treatment and distance from the camera showed that there were significant differences among light treatments in density ($p < 0.001$) with higher densities observed with RS illumination , and significant effects of distance from the camera ($p < 0.001$). There was a small decrease in density of small rockfish at distances < 75 cm, possibly indicating avoidance of the drop camera system at these close ranges (Fig. 8). In general, densities were greatest for small rockfish at distances from 50 cm to 175 cm. A change in fish density with range was observed for large rockfish (Fig. 8), although densities of large rockfish decreased after 125 cm for all lighting treatments. The effect of distance from the drop camera system was significant for large rockfish as well (p = 0.010), while the effect of light treatment was not significant (consistent with earlier analyses). For both small and large rockfish the interaction term between treatment and distance was not significant, indicating that the effect of distance was the same for all light treatments.

The distance off-seafloor measurements for 100 small rockfish sampled at random indicated that there were significant differences among light treatments. In the ANCOVA, the main effect (light treatment) and the covariate (distance from the camera) were both significant ($p < 0.001$ and p = 0.014). The height above the seafloor was significantly higher for small rockfish in the two strobe light treatments (RS and WS) than the CW treatment (Fig. 9). There was no difference between the two strobe light treatments. Additionally, small rockfish at a greater distance from the camera were observed higher off the seafloor than those closer to the camera (Fig. 9). The ANCOVA indicated that on average, a fish at 225 cm from the camera was likely to be about 20 cm higher off the seafloor than a fish observed 75 cm from the camera (Fig 9b). The interaction term was not significant indicating that fish height above bottom did not vary with light treatments as the camera approached.

There was also a significant effect of distance between the camera and the height of large rockfish above the seafloor ($p = 0.034$), with large rockfish observed at 225 cm distance on average about 15 cm higher off the seafloor than those observed at 75 cm distance (Fig. 9d). The light treatment and the interaction between light treatment and distance were not significant. The effect of light treatment on height above the seafloor was nearly significant ($p = 0.052$) and the height above the seafloor for large rockfish was highest for the RS treatment and lowest for the CW treatment (Fig. 9). When split out by species, Copper Rockfish tended to be observed higher off the seafloor than the other species of large rockfish, with the exception of a single yelloweye viewed 23 cm off the seafloor under constant white light (Fig. 10). Very few Vermillion Rockfish and Yelloweye Rockfish were observed (Fig 10).

4.1 Discussion

Infrared lighting is used widely in surveillance applications (e.g. for security or for wildlife trail cameras) as it is unobtrusive. Infrared lighting is far outside the visible spectrum of most fish species and has been previously used in some studies to compare fish behavior in terms of light avoidance, swimming behavior, or detectible response between red and white lights (Olla et al. 2000; Widder et al. 2005; Raymond and Widder 2007). Although it is largely invisible to fish, infrared light has the disadvantage of very high absorption in water, making realistic visual range of observation often limited to less than 1 m. This makes it unsuitable for studies where visual detection of fishes and identification to species is needed. For many fishes, red light (620 to 700 nm) is less visible than light of shorter light wavelengths because of diminished visual sensitivity in the red part of the spectrum. For fish residing at depths greater than 50 m, very little ambient light at red wavelengths is available due to rapid attenuation compared with green and blue wavelengths (450 to 550 nm).

In this study we used far-red spectrum light (660 nm), further reducing the potential detectability by fish while gaining increased penetration in the water column compared with infra-red light. In this way, far-red light is more useful for identifying and counting fishes unobtrusively. The major drawback of far-red light is also a decreased range relative to white light due to high attenuation of red light in seawater, but under the conditions experienced during this study, the reduction in range was only ~0.25 m. A second drawback to far-red light is the loss of any color information in the images. This can reduce detectability of fish and make species identification more difficult. Using the data collected during this study and given the large number of small rockfish that were unidentifiable even under white light, the impacts of red light to species identification could not be adequately tested here. It should be noted however, that all the larger rockfish species were identifiable under all lighting treatments.

The effect of light type on optically measured abundance was significant. There were more fish observed under red strobed light, presumably because the reduced visual stimulus produced by these lights resulted in weaker avoidance response in small rockfish. This is similar to other studies that have found more fish observed under red lighting than white lighting conditions. For example, Widder et al. (2005) observed relative abundances of sablefish were five times higher with red lights than with white lights. Even red lights in a spectral range that was detectible by the sablefish caused less of a startle reaction than white (full spectrum) lights. This is consistent with laboratory studies, where the effect of light on light avoidance behavior has been shown to vary with fish activity level (Ryer et al. 2009). An active predatory fish, such as sablefish was found to have a strong reaction to light stimuli, which may be a potential reason for the absence of sablefish in a camera survey designed to assess their abundance (Lauth et al. 2004).

A second result of the study with respect to lighting is the apparent differences between strobed and continuous lighting. Strobed lights are sometimes used as a deterrent for fish (e.g. McIninch and Hocutt, 2007), but this study did not record a negative response of strobed lighting relative to constant light. The strobe duration used in this study was relatively short (2 ms), and even at 4 frames per second, the continuous lights emitted substantially more light when integrated over time. This study suggests that the short duration of the strobes may not provide as strong a stimulus for fish avoidance relative to continuous lights, although this contrast was not significant, and was not as strong as the difference in light frequency. As the use of strobed light systems is likely to increase given the greater efficiency of LED strobes, more studies on the effect of strobed and continuous lights should be undertaken.

The effects of light on abundance observed in this study are most likely caused by changes in rockfish avoidance behavior in the presence of higher levels of detectable light. This effect depends on the species and sizes observed. Raymond and Widder (2007) found that sablefish reacted strongly to illumination with white and red lights and less strongly with far-red lights, while a species of grenadier in the same study did not react to any of these same lighting treatments. Similar species-specific reactions have been reported in other *in situ* studies. Krieger and Ito (1999) found that some species of rockfish responded to an approaching submarine by diving towards the seafloor, while others did not respond. In two species (rougheye rockfish, *Sebastes aleutianus* and shortraker rockfish, *S. borealis*) a different response was observed depending if the fish was first observed off the seafloor (diving response) or on the seafloor (no response). Similarly, Laidig et al. (2013) found that reactions to both manned submersibles and remotely operated vehicles could vary by species, with species that tended to aggregate in the water column having a much stronger reaction to an underwater vehicle than species that were always found near the seafloor. Many other researchers have recorded different reactions to underwater visual platforms by different sizes and species of fish (Lauth et al. 2004; Adams et al. 1995; Trenkel et al. 2004; Stoner et al. 2008).

In this study, we found a significant effect of distance from the camera on the measured density of fishes, with most fishes occurring from 75 to 200 cm from the camera for both small and large rockfish. This was likely driven by detectability rather than attraction to the camera. The effect was consistent across lighting treatments (the interaction term in the ANOVA was insignificant in both cases). This is consistent with a detectability function that decreases as the distance from the camera increases. In addition, we saw no evidence that fish were attracted to the camera in any of the deployments, such as fish moving towards the camera during the deployment.

Lighting is only one of the possible stimuli (lights, motion and noise) that fish in our study may have reacted to. The underwater camera frame was large (0.5 m by 0.5 m by 1.0 m) relative to the fishes we were observing; it undoubtedly interacted with the seafloor creating underwater noise, and the research vessel that was used to tow the drop camera was also a source of underwater noise which can cause reactions (De Robertis and Handegard, 2013). This highlights the need to understand reaction to the underwater survey platform and vessel as well as light. Differences in densities of rockfish observed along the same transects by different vehicles have been seen in other studies (Laidig et al. 2013) who found that 11% of rockfish responded to the manned submersible, while 57% of rockfish responded to the remotely-operated vehicle. These differences were attributed to different characteristics of the vehicles, one of which is the different lighting configurations between the manned submersible (starboard side lighting) and the remotely-operated vehicle (head-on lighting). There may also be interactions between the effects of lighting and other aspects of the survey platform or motion. For example, repeating this experiment with a stationary camera may yield different results, as lighting may influence how a fish perceives motion.

In summary, we detected a significant difference in fish abundance for small rockfish in the different light treatments. More light in the detectable range of rockfish led to fewer fish being observed during the deployments. On average, the number of small rockfish observed was reduced by half from strobed red light to strobed white light and by 75% from strobed red light to constant white light. There was also a significant reaction of moving closer to the seafloor by both large and small rockfish to the approaching camera. For small rockfish, the reaction was to move closer to the seafloor in the presence of brighter and constant lights, for large rockfish the effect of lighting treatment was not significant, but they appeared to respond to the approaching camera only. These findings have implications for underwater surveys of rockfish. Care should be taken whenever possible to minimize the overlap between light spectra emission and spectra that are visible to rockfish, so that the most accurate estimation of fish abundance can be obtained. For example, Jaffe et al. (1998) used red light to minimize behavioral reactions to lighting on an underwater imaging system (660 nm) for zooplankton. The implications of this study are that visible lights can decrease the observed density of fish during underwater camera surveys. Additionally, fish behavior and reaction to underwater platforms can be affected by the degree to which lighting regimes overlap spectral sensitivities of target fishes. Thus, care should be taken to account for and minimize these effects in the selection of underwater lighting in future studies and experiments.

The study conducted here is novel in that we attempted to isolate the effect of lighting regime on observable fish abundance and avoidance behavior through a rigorous experimental design to provide conclusive results. The effect of lighting on fishes response to underwater visual platforms has never been studied in the field using both conspicuous (white) and inconspicuous (far red) lighting. Given the results of this study, the effects of underwater lighting are of greater concern when examining small rockfish species, while the overall effect of the approaching platform (regardless of lighting regime) may be more important for studies examining large rockfish species. Although lighting is an important component of the stimuli associated with underwater visual survey platforms, further studies to examine other components is needed to determine the relative contribution of lighting to avoidance behavior in rockfishes.

5.1 Acknowledgments

The successful completion of the fieldwork was made possible by the assistance of D. Duggins, D. Willows, K. Kull and J. Fahlbusch of UW-Friday Harbor Laboratory and R. Pacunski of WDFW. R. Towler and J. Harms provided assistance with the underwater camera equipment. L.

Britt provided advice and expertise on underwater lighting. This manuscript was improved by discussions and comments from G.R. Hoff, C. Ryer, W. Palsson, D. Somerton, and two anonymous reviewers. This study was funded by NMFS Office of Science and Technology, Untrawlable Habitat Strategic Initiative.

6.1 References

Adams, P.B., Butler, J.L., Baxter, C.H., Laidig, T.E., Dahlin, K.A., and Wakefield, W.W. 1995. Population estimates of Pacific coast groundfishes from video transects and swept-area trawls. Fish. Bull., U.S. **93**: 446–455.

Auster, P.J., Lindholm, J., and Valentine, P.C. 2003. Variation in habitat use by juvenile Acadian redfish, *Sebastes fasciatus*. Environ. Biol. Fishes **68**: 381−389.

Bouguet, J.Y. 2008. Camera Calibration Toolbox for Matlab [online]. Available from vision.caltech.edu/bouguetj/calib_doc/index.html [accessed 20 September 2008].

Bowmaker, J.K. 1990. The visual pigments of fishes. *In* The visual system of fish. *Edited by* R. Douglas and M. Djamgoz. Chapman and Hall, London, UK. Pp. 81-107.

Brill, R., Magel, C., Davis, M., Hannah, R., and Rankin, P. 2008. Effects of rapid decompression and exposure to bright light on visual function in black rockfish (*Sebastes melanops*) and Pacific halibut (*Hippoglossus stenolepis*). Fish. Bull., U.S. **106**: 427-437.

De Robertis, A., and Handegard, N.O. 2013. Fish avoidance of research vessel and the efficacy of noise reduced vessels: A review. ICES J. Mar. Sci. **70**: 34-35.

Demer, D.A., Cutter, G.R., Renfree, J., and Butler, J.L. 2009. A statistical-spectral method for echo classification. ICES J. Mar. Sci. **66**: 1081-1090.

Douglas, R.H. and Hawryshyn, C.W. 1990. Behavioural studies of fish vision: an analysis of visual capabilities. *In* The visual system of fish. *Edited by* R. Douglas and M. Djamgoz. Chapman and Hall, London, UK. pp. 373-418.

Greene, H.G., Bizzarro, J.J., O'Connell, V.M., and Brylinsky, C.K. 2007. Construction of digital potential marine benthic habitat maps using a coded classification scheme and its application. In Todd, B.J., and Greene, H.G. (Eds.), Mapping the Seafloor for Habitat Characterization, Canadian Geological Association Special Paper **47**, p. 141-155.

Hixon, M.A., Tissot, B.N., and Pearcy, W.G. 1991. Fish assemblages of rocky banks of the Pacific Northwest. OCS Study MMS 91-0052, US Department of the Interior, Minerals Management Service, Camarillo, CA.

Jaffe, J.S., Ohman, M.D. and De Robertis, A. 1998. OASIS in the sea: measurement of acoustic reflectivity of zooplankton with concurrent optical imaging. Deep-Sea Res. II **45**: 1239-1253.

Jerlov, N. G. 1976. Marine Optics, Elsevier, New York. 231 pp.

Jones, D.T., Wilson, C.D., De Robertis, A., Rooper, C.N., Weber, T.C., and Butler, J.L. 2012. Evaluation of rockfish abundance in untrawlable habitat: combining acoustic and complementary sampling tools. Fish. Bull., U.S. **110**: 332-343.

Krieger, K.J., and Ito, D.H. 1999. Distribution and abundance of shortraker rockfish, *Sebastes borealis*, and rougheye rockfish, *S. aleutianus*, determined from a manned submersible. Fish. Bull., U.S. 97: 264-272.

Laidig, T.E., Krigsman, L.M., and Yoklavich, M.M. 2013. Reactions of fishes to two underwater survey tools, a manned submersible and a remotely operated vehicle. Fish. Bull., U.S. 112:54-67.

Lauth, R.R., Wakefield, W.W., and Smith, K. 2004. Estimating the density of thornyheads, *Sebastolobus* spp., using a towed video camera sled. Fish. Res. **70**: 39-48.

Lorance, P. and Trenkel, V.M. 2006. Variability in natural behaviour and observed reactions to an ROV, by mid-slope fish species. J. Exp. Mar. Biol. Ecol. **332**: 106-119.

Love, M.S., Yoklavich, M., and Schroeder, D.M. 2009. Demersal fish assemblages in the Southern California Bight based on visual surveys in deep water. Environ. Biol. Fishes **84**: 55–68.

McIninch, S.P., and Hocutt, C.H. 1987. Effects of turbidity on estuarine fish response to strobe lights. J. Applied Ichthyology **3**: 97–105.

O'Connell, V.M., and Carlile, D.W. 1993. Habitat-specific density of adult yelloweye rockfish *Sebastes ruberrimus* in the eastern Gulf of Alaska. Fish. Bull., U.S. **91**: 304-309.

O'Connell, V.M., and D.W. Carlile. 1994. Comparison of a remotely operated vehicle and a submersible for estimating abundance of demersal shelf rockfish in the eastern Gulf of Alaska. N. Am. J. Fish. Manage. **14**: 196-2.

Olla, B.L., Davis, M.W., and Rose, C. 2000. Differences in orientation and swimming of walleye pollock, *Theragra chalcogramma*, in a trawl net under light and dark conditions: Concordance between field and laboratory observations. Fish. Res. **44**: 261-266.

R Core Development team. 2013 R: A language and environment for statistical computing. R Foundation for Statistical Computing, Vienna, Austria. ISBN 3-900051-07-0, URL http://www.R-project.org.

Raymond, E.H., and Widder, E.A. 2007. Behavioral responses of two deep-sea fish species to red, far-red, and white light. Mar. Ecol. Prog. Ser. **350**: 291-298.

Ressler, P.H., Fleischer, G.W., Wespestad, V.G, and Harms, J. 2009. Developing a commercial-vessel-based stock assessment survey methodology for monitoring the U.S. West Coast widow rockfish (*Sebastes entomelas*) stock. Fish. Res. **99**: 63-73.

Rooper, C.N., Hoff, G.R. and De Robertis, A. 2010. Assessing habitat utilization and rockfish (*Sebastes* sp.) biomass in an isolated rocky ridge using acoustics and stereo image analysis. Can. J. Fish. Aquat. Sci. **67**: 1658-1670.

Ryer, C.H., Stoner, A.W., Iseri, P.J., and Spencer, M.L. 2009. Effects of simulated underwater vehicle lighting on fish behavior. Mar. Ecol. Prog. Ser. **391**: 97-106.

Stein, D.L., Tissot, B.N., Hixon, M.A., and Barss, W. 1992. Fish-habitat associations on a deep reef at the edge of the Oregon continental shelf. Fish. Bull., U.S. **90**: 540-551.

Stoner, A.W., Ryer, C.H., Parker, S.J., Auster, P.J., and Wakefield, W.W. 2008. Evaluating the role of fish behavior in surveys conducted with underwater vehicles. Can. J. Fish. Aquat. Sci. **65**: 1230–1243

Stone, R.P. 2006. Coral habitat in the Aleutian Islands off Alaska: Depth distribution, fine-scale species associations, and fisheries interactions. Coral Reefs **25**: 229-238.

Stierhoff, K.L., Butler, J.L., Mau, S.A., and Murfin, D.W. 2013. Abundance and biomass estimates of demersal fishes at the Footprint and Piggy Bank from optical surveys using a remotely operated vehicle (ROV). NOAA-TM-NMFS-SWFSC-521. US Department of Commerce, Technical Memorandum, Southwest Fisheries Science Center, La Jolla, CA.

Trenkel, V.M., Lorance, P., and Mahevas, S. 2004. Do visual transects provide true population density estimates for deepwater fish? ICES J. Mar. Sci. **61**: 1050-1056.

Widder, E.A., Robison, B.H., Reisenblichler, K.R. and Haddock, S.H.D. 2005. Using red light for in situ observations of deep-sea fishes. Deep-Sea Res. **52**: 2077-2085.

Williams, K., Rooper, C.N., and Towler, R. 2010. Use of stereo camera systems for assessment of rockfish abundance in untrawlable areas and for recording pollock behavior during midwater trawls. Fish. Bull., U.S. **108**: 352-362.

Xu G., and Zhang, Z. 1996. Epipolar geometry in stereo, motion, and object recognition: a unified approach, 336 p. Kluwer Academic Publs., Norwell, MA.

Yoklavich, M.M., Love, M.S., and Forney, K.A. 2007. A fishery-independent assessment of an overfished rockfish stock, cowcod (*Sebastes levis*), using direct observations from an occupied submersible. Can. J. Fish. Aquat. Sci. **64**: 1795-1804.

7.1 Tables

Table 1. Average range (r) for each treatment (and standard error) and corresponding total volume observed per frame and overlapping volume per frame used to compute densities.

Treatment	Mean range (cm)	Total volume (m^3)	Overlapping volume (m^3)
Red strobe lights	225 (7.7)	7.54	2.72
White strobe lights	252 (6.4)	10.48	3.91
White constant lights	243 (9.3)	9.44	3.49

Table 2. Counts of species observed in categories (large rockfish and small rockfish) for each lighting treatment. The percentage of each species group occurring in rocky habitats is also shown.

Grouping	Species or taxa name	Total count			
		Red strobe light	White strobe light	White constant light	Percent in rocky habitat
Small rockfishes	Puget Sound rockfish	602	351	94	89%
	Harlequin rockfish	12		5	
	Unidentified rockfish	1779	1156	537	
Large rockfishes					96%
	Copper rockfish	48	49	42	
	Quillback rockfish	15	22	30	
	Vermillion rockfish			4	
	Yelloweye rockfish	10		3	

Table 3. Results of analyses (ANOVA and ANCOVA) testing for the effects of lighting treatment on rockfish density and behavior. The dependent variable for each analysis is given, as well as the factors included in the analyses as independent variables. Degrees of freedom (df), F-values, residual mean-squared-error (MSE), and p-values are given for all analyses.

Dependent variable	Factor/Error	df	F-value/MSE	p value	
Small rockfish density	Block	10	3.641	0.007	*
	Treatment	2	7.104	0.005	*
	Error	20	1.37E-04		
Large rockfish density	Block	10	1.062	0.433	
	Treatment	2	0.670	0.523	
	Error	20	1.36E-06		
Maximum number of rockfish	Block	10	3.27	0.012	*
	Treatment	2	8.68	0.002	*
	Error	20	1.61E+01		
Small rockfish density	Block	9	16.688	<0.001	*
	Treatment	2	17.633	<0.001	*
	Distance from camera	6	8.064	<0.001	*
	Treatment*Distance	12	1.664	0.078	
	Error	189	1.15E-02		
Large rockfish density	Block	9	0.958	0.478	
	Treatment	2	2.807	0.064	
	Distance from camera	6	2.975	0.010	*
	Treatment*Distance	12	0.652	0.794	
	Error	133	3.93E-05		
Small rockfish height off the seafloor	Treatment	2	29.821	<0.001	*
	Distance from camera	1	6.07	0.014	*
	Treatment*Distance	2	2.827	0.061	
	Error	294	5.35E+02		
Large rockfish height off the seafloor	Treatment	2	3.088	0.052	
	Distance from camera	1	4.676	0.034	*
	Treatment*Distance	2	1.01	0.370	
	Error	65	3.16E+02		

*indicates statistical significance ($p < 0.05$)

8.1 Figures

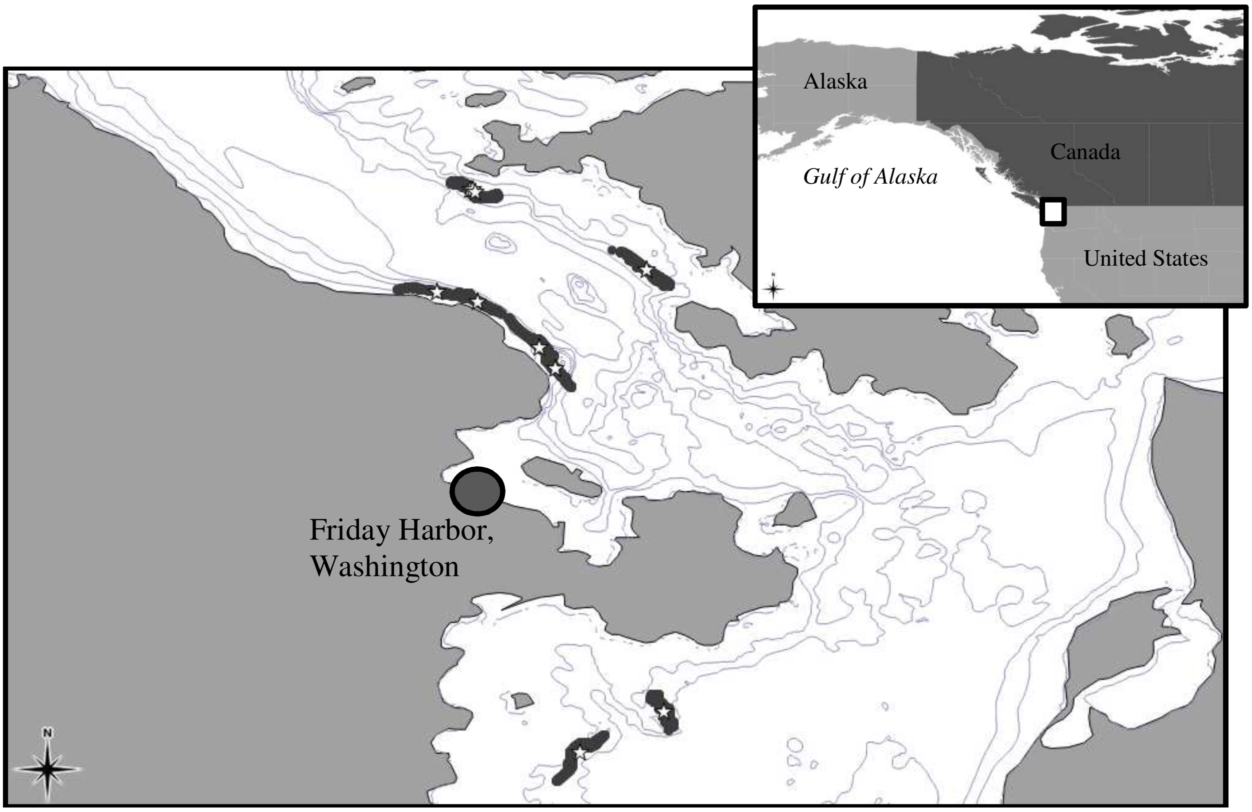

Fig. 1. Map of study area near Friday Harbor, Washington, showing the transects (n = 11) where three deployments were conducted (one for each light treatment). Stars indicate the center point of each transect, the grey areas show the full extent of the transects. The northernmost grey area contained 4 closely spaced transects. Four transects were spaced end to end in the grouping just north of Friday Harbor.

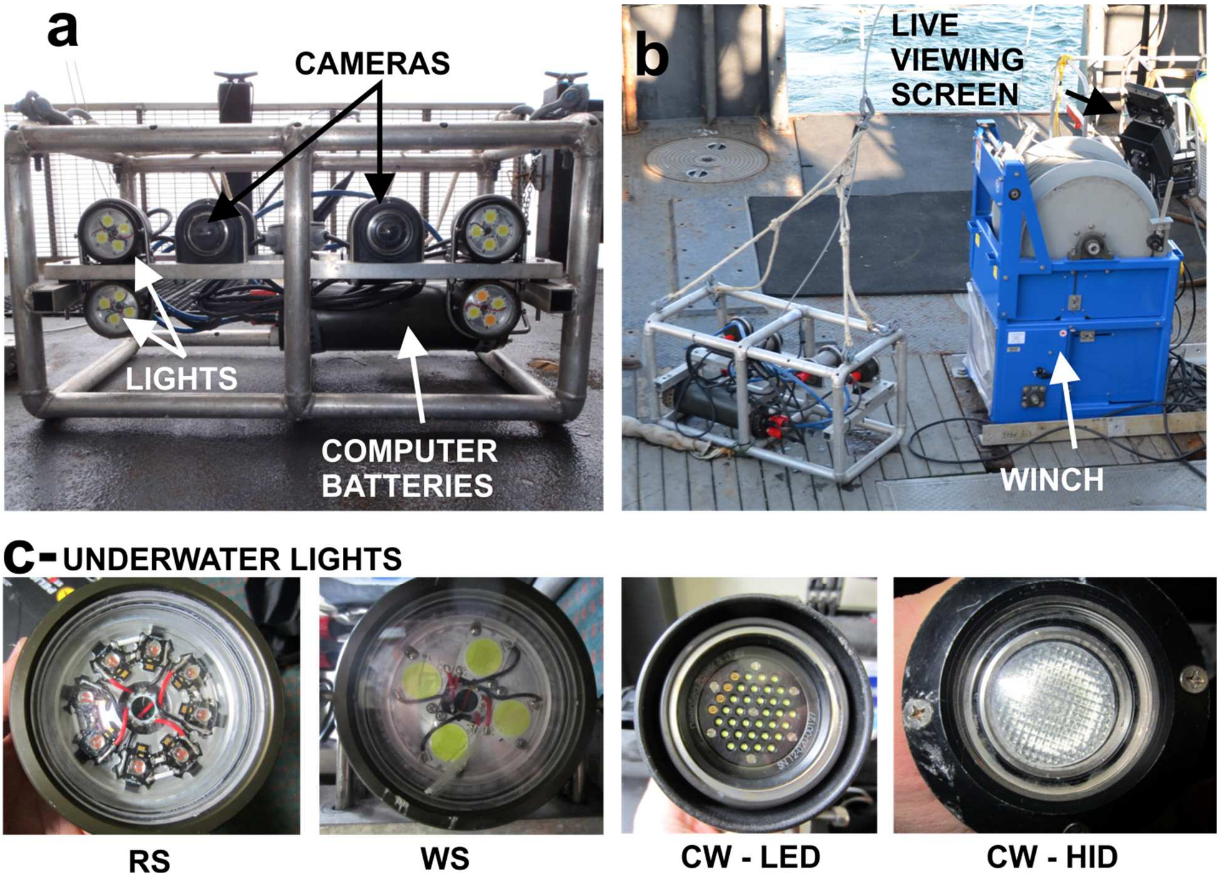

Fig. 2. Stereo drop camera system that was towed or drifted along transects (a) with the quick responding electric winch (b), and insets of each underwater lighting type and corresponding treatment (c). RS is red strobed light, WS is white strobed light, CW-LED is constant white light (light emitting diode) and CW-HID is constant white light (high intensity discharge).

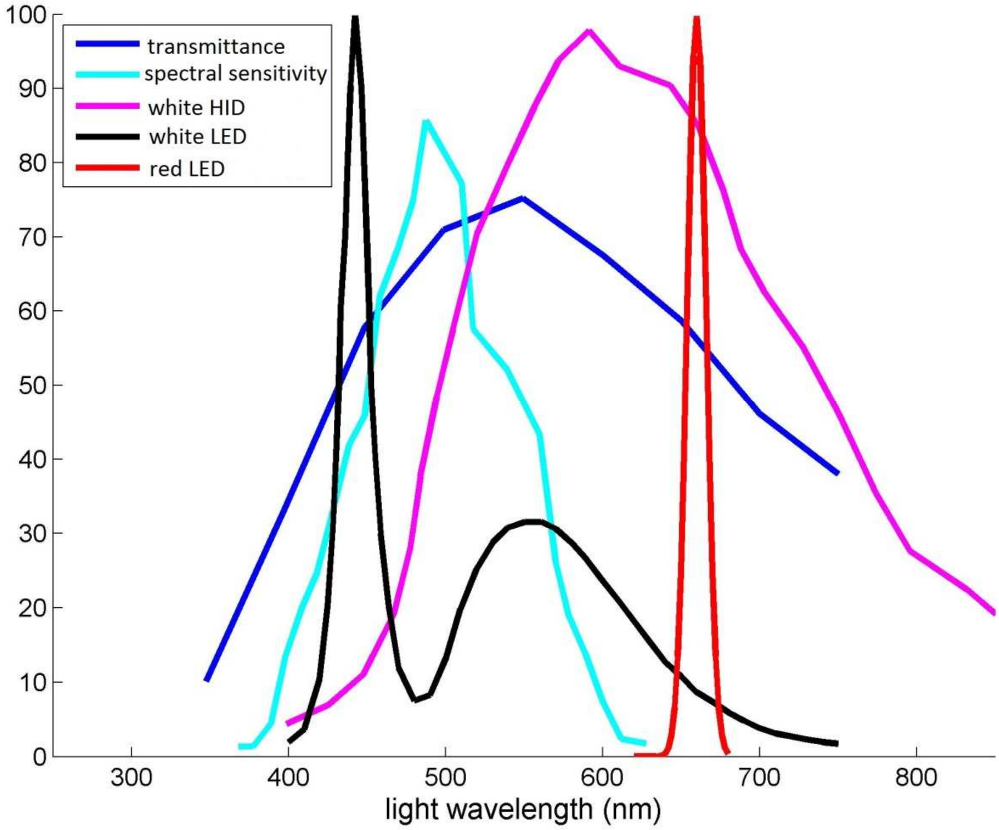

Fig. 3. Spectral sensitivity of black rockfish (*Sebastes melanops*) from Brill et al. (2008), approximate transmittance properties of coastal seawater (Jerlov, 1976) and spectral profile of each of the three lighting types (red LED light, white LED light, and white HID light).

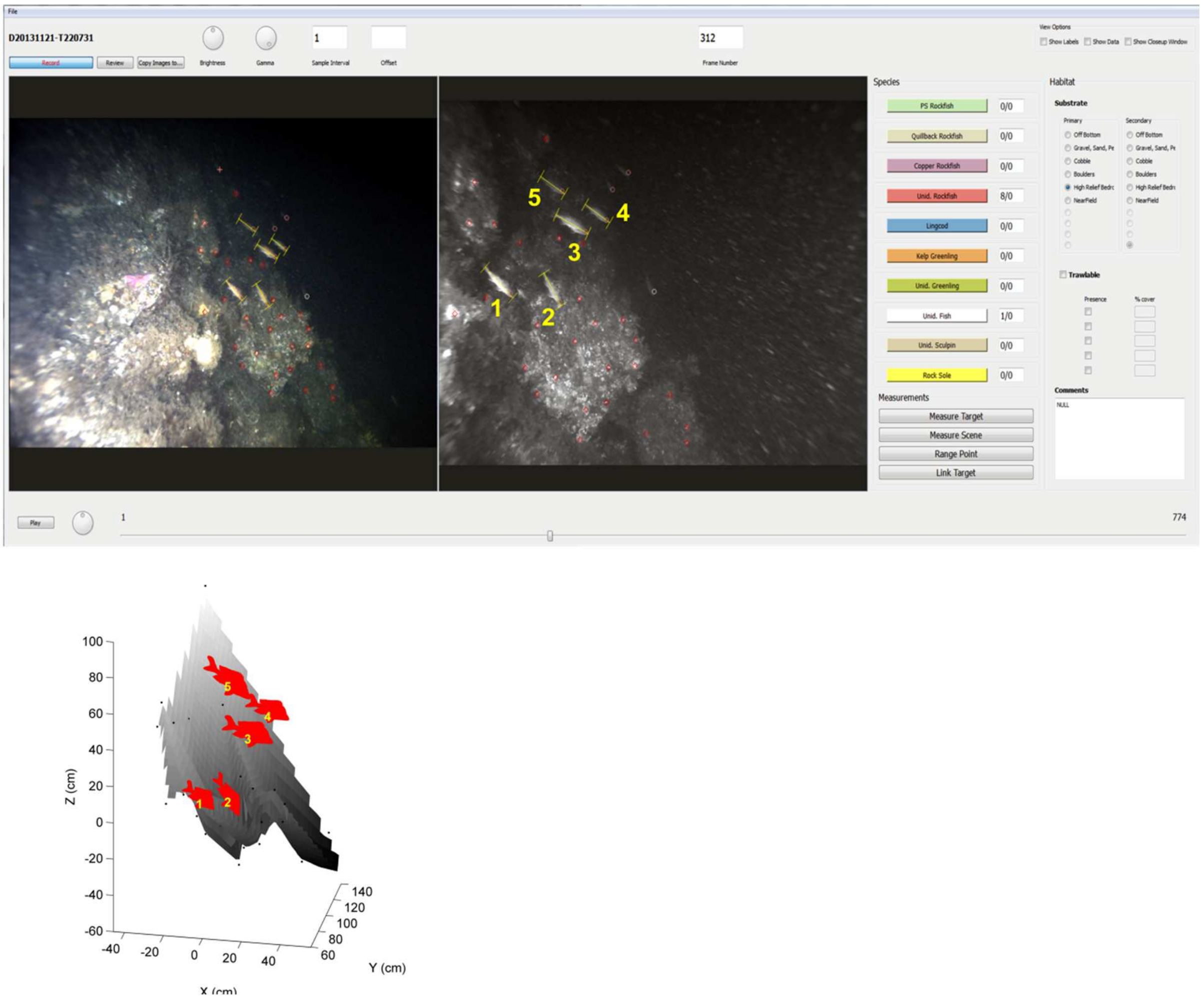

Fig. 4. Stereo measurement software interface showing five rockfish viewable in both images that were measured using stereo techniques (upper panel). The lower panel shows the 3-dimensional reconstruction of the measured images, as well as a 3-dimensional reconstruction of the seafloor computed from the ranges at the red dots in the upper panel.

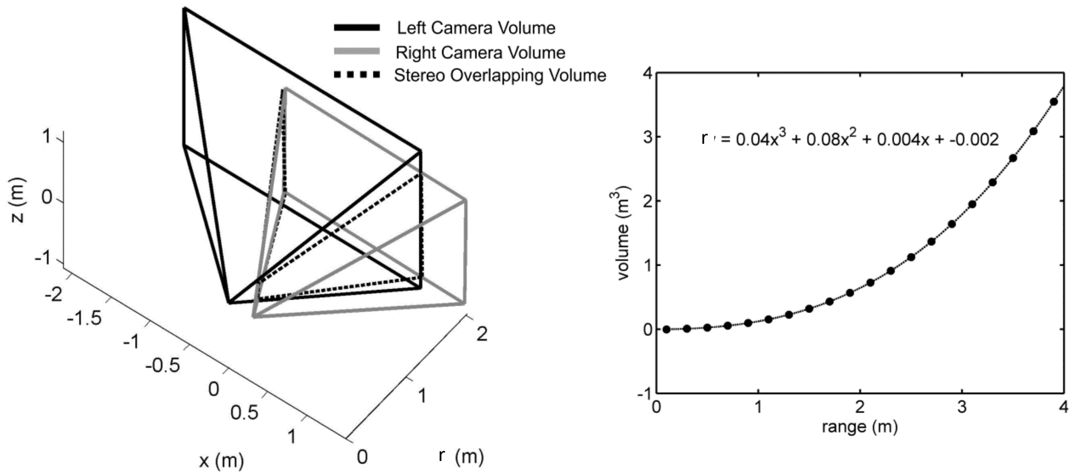

Fig. 5. Projection of the field of view for the left and right camera and their overlapping volumes (left panel) and the overlapping volume of the left and right cameras as a function of range (r) from the camera (right panel).

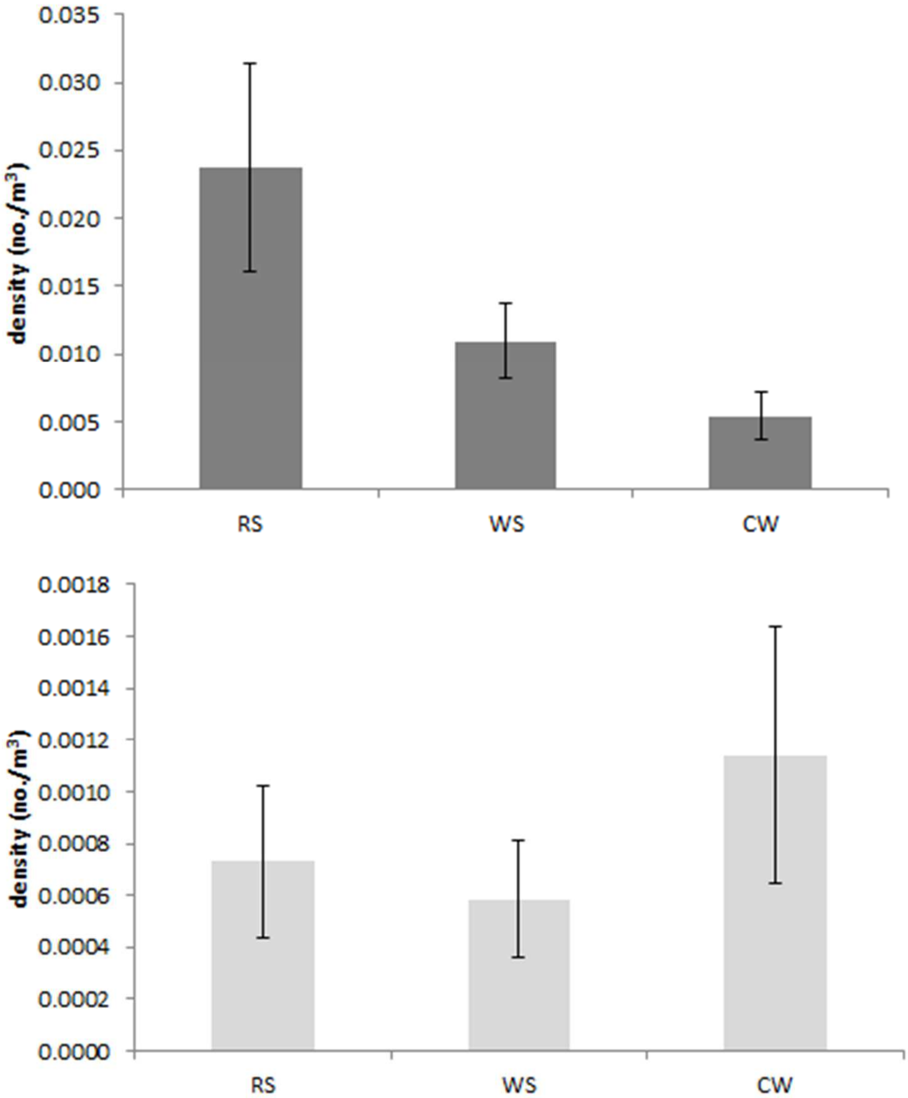

Fig. 6. Volumetric density estimates for small rockfish (Puget Sound, and unidentified; top panel) and large rockfish (Quillback, Copper, Yelloweye and Vermillion; bottom panel) by light treatment (RS, red strobe light; WS, white strobe light; CW, constant white light). Standard error bars are shown.

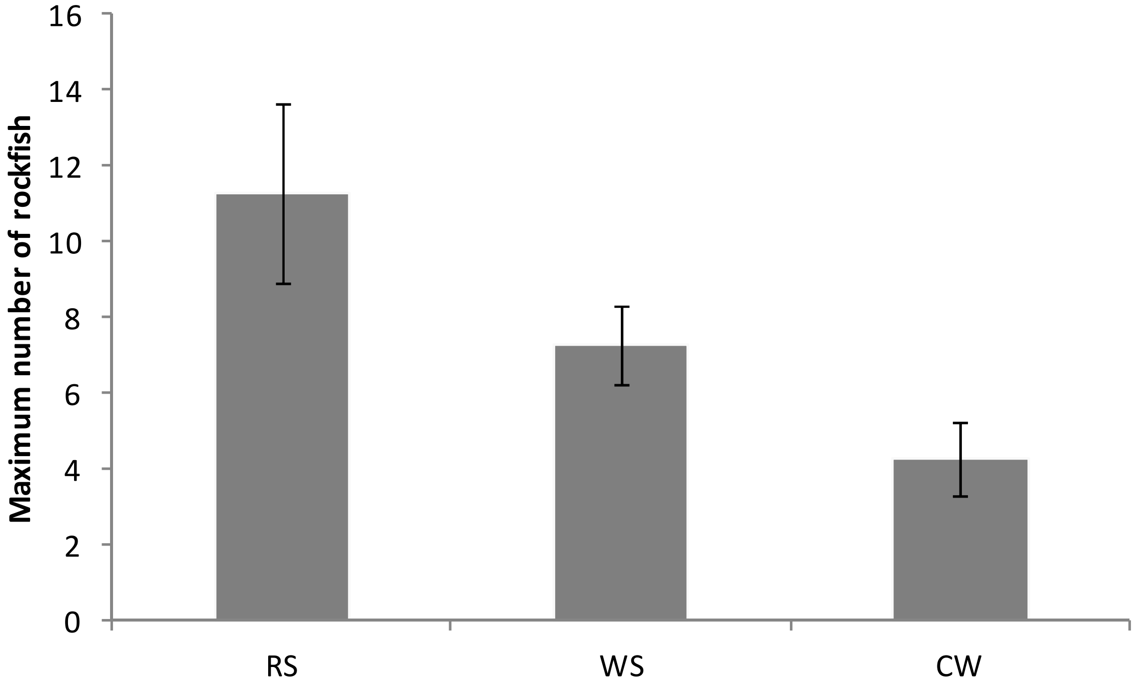

Fig. 7. Average (across camera drops) maximum number of rockfish in a single frame for each of the three treatments (RS, red strobe light; WS, white strobe light; CW, constant white light). This comparison was significant ($p = 0.0187$) and post-hoc test indicated only RS and CW were significantly different from each other. Standard error bars are shown, $n = 11$ transects per treatment.

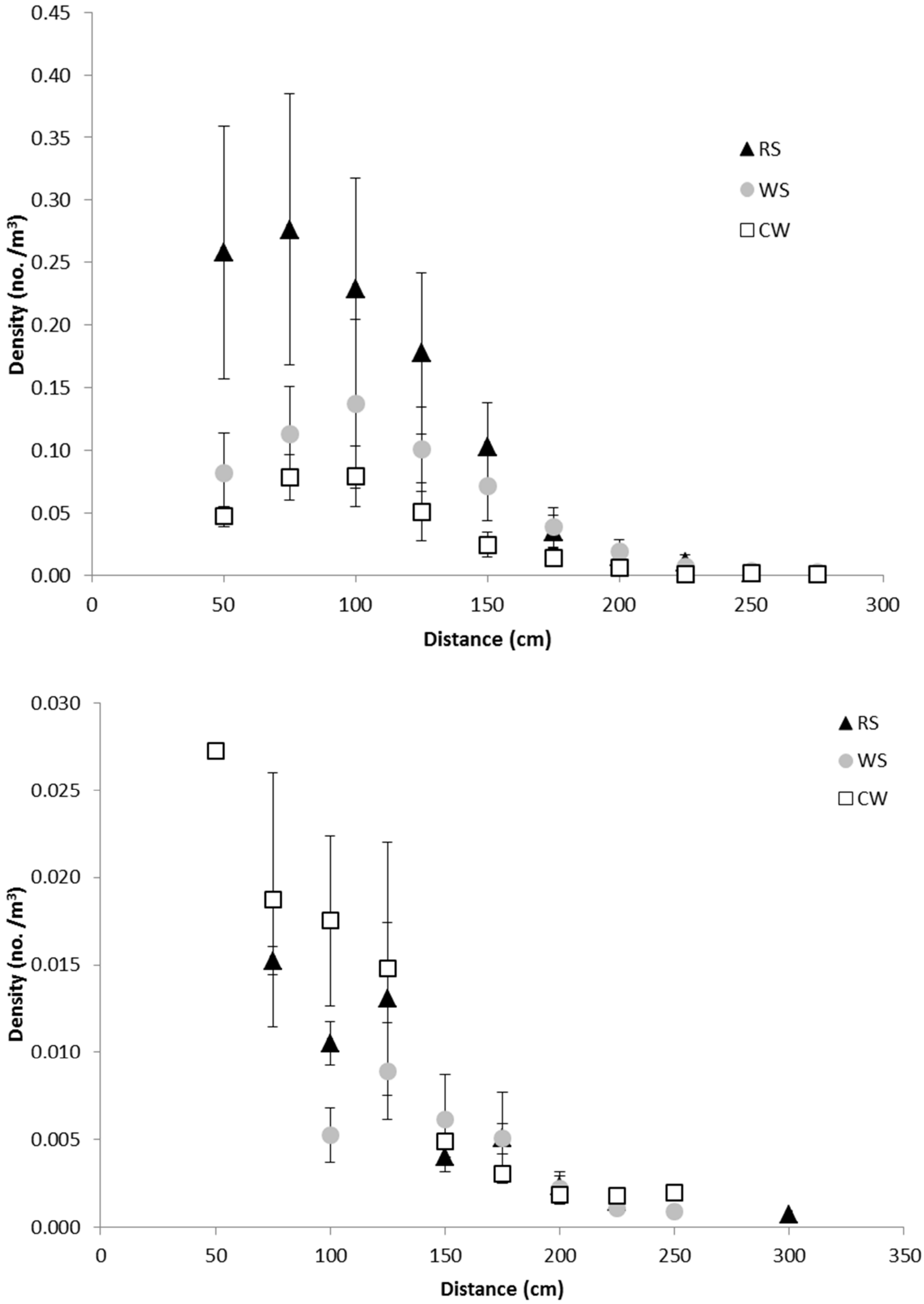

Fig. 8. Density of small rockfish (top panel) and large rockfish (bottom panel) by distance from the drop camera system averaged across deployments in 25 cm bins from the drop camera,

shown by treatment (RS, red strobe light; WS, white strobe light; CW, constant white light). Standard errors are shown.

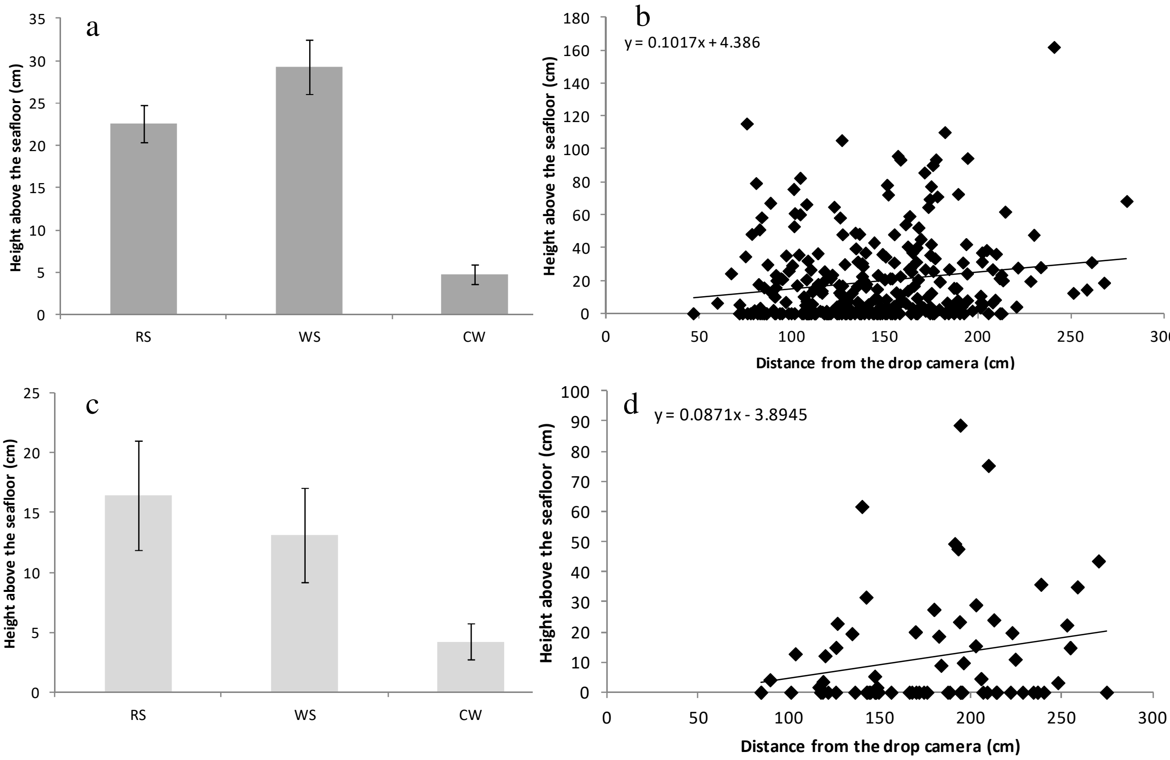

Fig. 9. Mean height above the seafloor (and standard error) for small rockfish by lighting treatment (a), height above the seafloor for small rockfish as a function of distance from the camera (b), height above the seafloor for large rockfish by lighting treatment (c), and height above the seafloor for large rockfish as a function of distance from the camera (d). RS = red strobe light; WS = white strobe light and CW = constant white light.

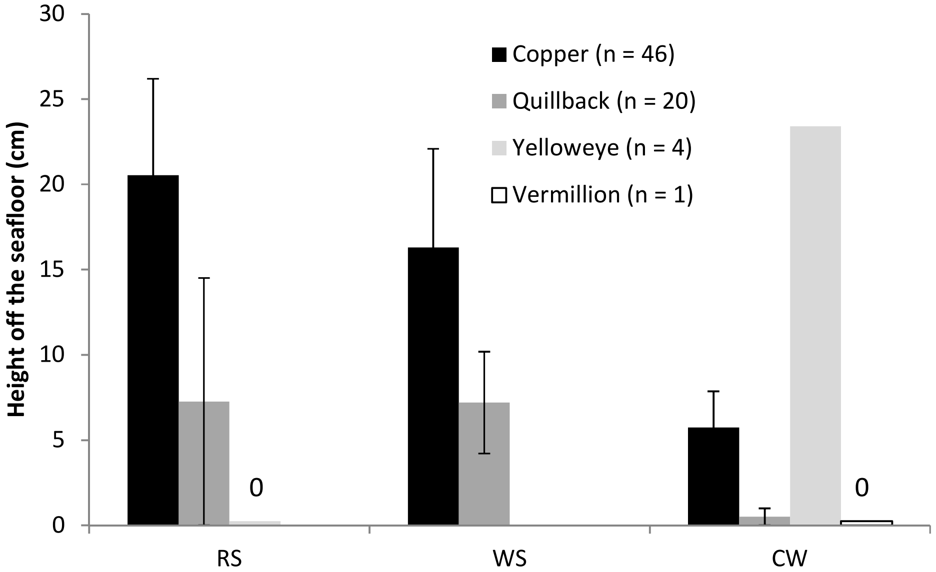

Fig. 10. Mean height off the seafloor (and standard error) by species and lighting type (RS, red strobe light; WS, white strobe light; CW, constant white light) for large rockfish species. Zero indicates the height above the seafloor was 0 cm.